IET Communications

Research Article

IET Journals
The Institution of Engineering and Technology

Bio-inspired collaborative spectrum sensing and allocation for cognitive radios

ISSN 1751-8628
Received on 15th August 2014
Revised on 12th May 2015
Accepted on 23rd June 2015
doi: 10.1049/iet-com.2014.0769
www.ietdl.org

Freeha Azmat ✉, *Yunfei Chen*, *Nigel Stocks*

School of Engineering, University of Warwick, Coventry, CV4 7AL, UK
✉ *E-mail: F.Azmat@warwick.ac.uk*

Abstract: Bio-inspired techniques, including firefly algorithm, fish school search, and particle swarm optimisation, are utilised in this study to evaluate the optimal weighting vectors used in the data fusion centre. This evaluation is performed for more realistic signals that suffer from non-linear distortions, caused by the power amplifiers. The obtained optimal weighting vectors are then used for collaborative spectrum sensing and spectrum allocation in cognitive radio networks. Numerical results show that bio-inspired techniques outperform the conventional algorithms used for spectrum sensing and allocation by deriving optimal weights that ensure the highest value of probability of detection and guarantee the maximum proportional fair reward for users.

1 Introduction

In collaborative spectrum sensing (CSS) with energy detection, a data fusion centre combines energy measurements from all collaborating cognitive radios (CRs) to make a final detection decision. It was observed in [1] that collaborative scheme outperforms the standalone energy detector. Chavali and Dasilva [2] derived optimal and sub-optimal weights for a linear combination of measurements in the data fusion centre. More works on spectrum sensing can be found in [3] and the references therein.

After spectrum sensing, spectrum allocation is often performed to allocate the detected channels. A common method used for spectrum allocation is colour-sensitive graph colouring (CSGC) [4]. In this method, the spectrum allocation model is translated into a graph colouring problem, but an issue with the CSGC algorithm was that the execution time increases, when the number of channels increases. In [5], a parallel algorithm for spectrum allocation was presented. It achieves the same spectrum allocation benefits as the CSGC algorithm, but with less execution time. However, it cannot ensure the secondary user access fairness. In this paper, a CSS and allocation framework is proposed using bio-inspired techniques which not only provides an optimal weighting vector for data fusion centre, but also ensures secondary user access fairness.

i. Three bio-inspired algorithms: firefly algorithm (FFA), fish school search (FSS), and particle swarm optimisation (PSO) are used in this paper, where FFA and FSS have not been used for both CSS and allocation before. It will be shown that FFA and FSS algorithm outperform previous algorithms for both CSS and allocation scenarios.
ii. In previous works, linear primary user signals were considered. However, in reality, primary user signals may suffer from non-linear distortions, that is, if the power amplifier (PA) does not have enough gain, the input of the PA at the primary user will be non-linearly distorted. In this case, the linear weights of the measurements as used in [2] may not be optimal any more. So, we have considered both linear and non-linear primary input signals with interference and fading losses in this paper.
iii. For CSS, the optimal 'weighting vector' in the data fusion centre is computed using the popular algorithm 'weighted linear combining (WLC)' [2], and numerical results in this paper will show that the bio-inspired algorithms outperforms the WLC method.
iv. We have proposed a spectrum allocation approach which is dependent on optimal 'weighting vector' evaluated by the data fusion centre. The relationship between the optimal 'weighting vector' computed during CSS and the spectrum allocation module is not present before.

The rest of the paper is organised as follows. The system model is presented in Section 2 while the description of the spectrum sensing and spectrum allocation modules using bio-inspired techniques is presented in Section 3. Section 4 deals with the numerical results and discussion. Finally, conclusions are given in Section 4.

2 System model

In CSS, the binary hypothesis test is formulated as

$$H_0: r_d(m) = z_d(m) \tag{1}$$

$$H_1: r_d(m) = G_d s(m) + z_d(m). \tag{2}$$

In (1) and (2), $d = 1, 2, \ldots, D$ and $m = 1, 2, \ldots, M$, where D is the total number of radios and M is the total number of samples at each CR. Also, $r_d(m)$, $s(m)$, G_d, and $z_d(m)$ represent the received signal, the primary signal, the channel gain, and the zero-mean additive white Gaussian noise with variance $\sigma^2_{z_d}$, respectively. Both flat fading and frequency selective gains are considered. The frequency selectivity assumes the tapped delay line model given in [6]. The primary signal $s(m)$ is a non-linear signal where the non-linearity is induced by passing the signal through the PA at the primary user. Consider two amplitude variation (AM)/ amplitude variation (AM) conversion methods for memory less systems. They are as follows:

Memory less polynomial model: As explained in [7], a strictly memory-less PA can be described in pass band as a non-linear function that maps the real valued input to the real valued output. This memory-less non-linearity can be approximated by a power series as

$$s(m) = \sum_{p=1}^{P} b_p [I(m)]^p \tag{3}$$

where b_p are the real-valued coefficients, $I(m)$ is the pass-band PA

input, and $s(m)$ is the pass-band PA output signal in (3) that will be sampled by CR.

High PA (HPA) model: The non-linear HPA model in the transmitter represents the non-linear distortion imposed on the signal. A useful non-linear HPA model is the Saleh model [8, 9]. Utilising the Saleh model, the output of the HPA $s(m)$ is given by

$$s(m) = \frac{I(m)A(r_s)\,\mathrm{e}^{\mathrm{j}\phi(r_s)}}{r_s}. \tag{4}$$

In (4), $A(r_s)$ is an odd function of r_s, with a leading term representing AM/AM conversion and $\phi(r_s)$ is an even function of r_s, with a quadratic leading term representing AM/PM conversion. As AM/AM conversion is considered in this paper only, $\phi(r_s)$ is not taken into account. In (4), $r_s = |I(m)|$ and

$$A(r_s) = \frac{e_A r_s}{1 + f_A r_s^2}$$

where e_A and f_A are constants [9].

For spectrum sensing, the dth CR calculates its received signal energy by using

$$E_d = \sum_{m=0}^{M-1} |r_d(m)|^2$$

and sends it to the fusion centre. The fusion centre evaluates an output for decision as

$$y_{dd} = \sum_{d=0}^{D-1} w_d E_d = w^{\mathrm{T}} \boldsymbol{E}$$

where $\boldsymbol{E} = [E_1, E_2, \ldots, E_D]$ and $\boldsymbol{w} = [w_1, w_2, \ldots, w_D]^{\mathrm{T}}$ represents the weighting vector. The probability of detection (P_{d}) is derived as [10]

$$P_{\mathrm{d}} = Q\left(\frac{Q^{-1}(P_{\mathrm{f}})\sqrt{w^{\mathrm{T}} X_1 w} - ME_s G_d^{\mathrm{T}} w}{\sqrt{w^{\mathrm{T}} X_2 w}}\right) \tag{5}$$

where

$$Q(x) = \int_x^{\infty} \frac{1}{\sqrt{2\pi}} \mathrm{e}^{-t^2/2}\,\mathrm{d}t,\ P_{\mathrm{f}}$$

is the probability of false alarm, $\boldsymbol{X}_1 = 2M\mathrm{diag}^2(\sigma_{z_d})$, $\boldsymbol{X}_2 = 2M\mathrm{diag}^2(\sigma_{z_d}) + 4E_s\mathrm{diag}(G_d)$, $E_s = \sum_{m=0}^{M-1} |s(m)|^2$, $\boldsymbol{\sigma}_{z_d} = [\sigma_{z_1}^2, \sigma_{z_2}^2, \ldots, \sigma_{z_D}^2]$, $\boldsymbol{G}_d = [|G_1|^2, |G_2|^2 \cdots |G_D|^2]$, and diag() represent the diagonal matrices.

It is evident in (5) that P_{d} resulting from CSS can be optimised by optimising the weighting vector $\boldsymbol{w}$. Therefore, P_{d} is a function of $\boldsymbol{w}$, or $f(\boldsymbol{w}) = P_{\mathrm{d}}(\boldsymbol{w})$.

We have used three bio-inspired techniques for optimising $\boldsymbol{w}$, where $\boldsymbol{w}$ represents the position of bio-creature in our system. The motivation of using bio-inspired algorithms comes from 'foraging', where every bio-creature tries to detect the best location of food with the help of their mates. We have related the 'high food concentration' concept of bio-creatures to the 'high value of P_{d}' and the 'positions of bio-creatures' as the 'weighting vector'. We have referred the bio-creatures (fire flies, fishes, and birds) as particles in further explanation.

We assume a slow changing spectrum access of primary users and m as the particle which represents a sample sensed by CRs. A particle m has a specific position in D dimensions, where dimensions are assumed equal to the number of CRs as illustrated in Table 1 and shown in Fig. 1. Each optimal weighting vector $\boldsymbol{w} = [w_1, w_2, \ldots, w_D]^{\mathrm{T}}$ has D dimensions, where the value of each dimension, say w_D, represents the weight assigned to dth CR.

Table 1 Analogies between CRN framework and proposed bio-inspired techniques

Analogies between CRN and bio-inspired techniques	
CRN	Bio-inspired techniques
number of samples sensed by CR	number of particles
number of CRs	number of dimensions of the position of the mth particle
fitness function: P_{d}	fitness function: food concentration
optimal weighting vector	best position of particle with maximum fitness value

The weight for each CR determines its priority over the other, so we call it as 'priority weight'. It is evident that the change in particle's position will consequently affects the priority weights of all CR's in the system. During spectrum sensing, the fusion centre evaluates the optimal position of the particle that yields highest P_{d}. Once optimal $\boldsymbol{w}$ is known by CR, the spectrum allocation is performed by the fusion centre as shown in Fig. 1. During spectrum allocation, we propose that the frequency channels will be allocated according to the value of 'priority weights' in optimal w. Let w_1 and w_2 be two values of priority weights in optimal $\boldsymbol{w} = [w_1, w_2, \ldots, w_D]^{\mathrm{T}}$, where $w_1 > w_2$, which shows that priority will be given to CR1 compared to CR2. Spectrum allocation is explained in detail in Section 3.2.

We will use P_{d} in (5) as an objective function for the evaluation of both bionic spectrum sensing and bionic spectrum allocation metrics. In the literature, the optimal value of $\boldsymbol{w}$ was determined in three ways: equal gain combining (EGC), WLC, and optimal combining (OC) [2]. In these techniques, it was observed that WLC and OC outperform the EGC method because their received energy measurements are 'weighted' as shown in {[2], (5)] and [2], (7)}. To determine the optimal weighting vector in the WLC method, a heuristic technique was proposed in [10] that minimises the probability of detection error as

$$\boldsymbol{w}_{\mathrm{wlc}} = \frac{\gamma_{\mathrm{d}}}{1 + 2\gamma_{\mathrm{d}}} \tag{6}$$

where $\gamma_{\mathrm{d}} = \left(E_s|G_d|^2/\sigma_{z_d}^2\right)$ is signal-to-noise ratio (SNR) and $\boldsymbol{w}_{\mathrm{wlc}}$ represents the weight for each dth radio, respectively. Though WLC outperforms EGC, the proposed bio-inspired algorithms will perform better for the case of both linear and non-linear signals as will be explained in Section 4.

3 Proposed algorithms and methodology

We have used bio-inspired metaheuristic algorithms for the CSS and allocation in our approach, where metaheuristic algorithms are iterative search processes that efficiently perform the exploration and exploitation in the solution space for efficiently finding the near optimal solutions. In this context, three types of bio-inspired meta-heuristics PSO, FSS, and FFA were devised to find the optimal solutions of noisy non-linear continuous mathematical models. FFA is potentially more powerful in solving noisy non-linear optimisation problems. The FFA not only includes the self-improving process with the current space, but it also includes the improvement in its own space from the previous stages. In [11], it was evaluated using benchmark functions that FFA outperforms the PSO in noisy situations and in the problems with many local optima. PSO is a powerful optimisation tool but sometimes it cannot tackle dynamic optimisation problems. It occurs because the entire swarm often increases the exploitation around a good region of the search space, reducing the overall diversity of the population. In this regard, the FSS algorithm is considered which is capable of auto-regulating the exploration-exploitation trade-off compared to PSO [12]. The

IET Commun., 2015, Vol. 9, Iss. 16, pp. 1949–1959

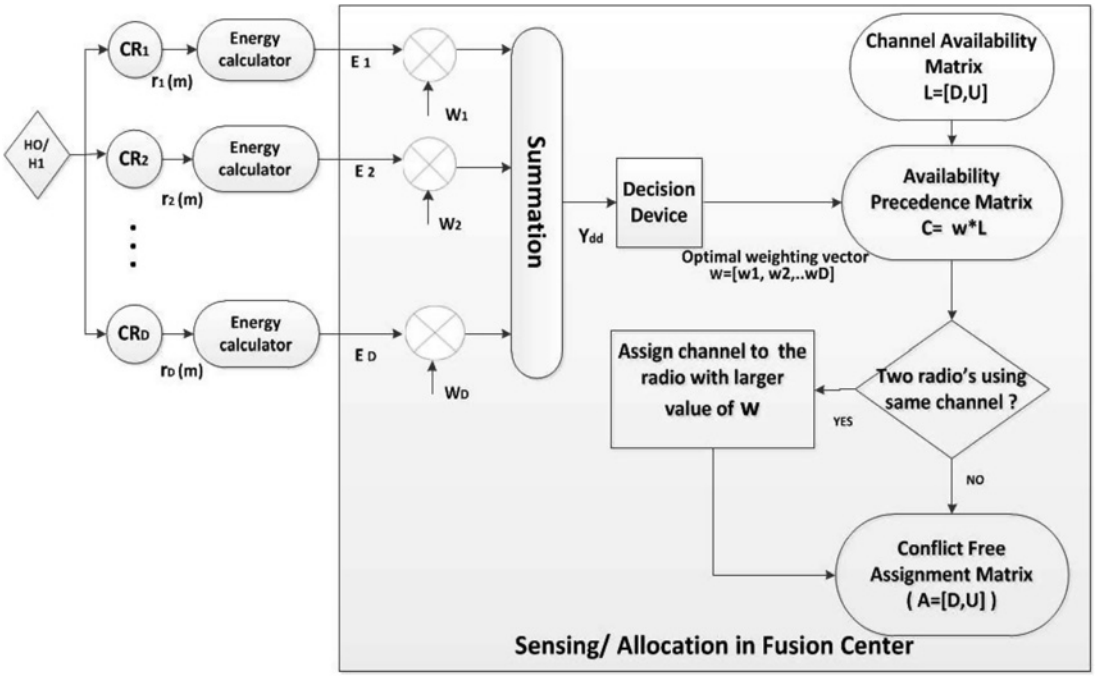

Fig. 1 *Centralised infrastructure that contains CSS and allocation framework*

proposed spectrum sensing and allocation using bio-inspired algorithms is given as follows:

3.1 Spectrum sensing

Let $\boldsymbol{w}_m^k = [w_{m1}^k, w_{m2}^k, \ldots, w_{mD}^k]$, where $\boldsymbol{w}_m^k$ represents the mth particle during iteration k in D dimensions, where $m = 1, 2, \ldots, M$ and M represents the total number of particles. The optimised $\boldsymbol{w}_m^k$ is evaluated using three bio-inspired techniques in this approach where first two steps are common in each algorithm given as

Step 1: Set $k = 0$, and generate initial positions of particles as $\boldsymbol{w}_m^k \epsilon a$, where a is a uniform random variable between [0,1].
Step 2: Evaluate the fitness of each particle ($P_{\mathrm{d}}(\boldsymbol{w}_m^k)$) using objective function in (5).
Step 3: This step is specific for each technique and explained below.
i. FFA:
(a) If ($P_{\mathrm{d}}(\boldsymbol{w}_2^k) > P_{\mathrm{d}}(\boldsymbol{w}_1^k)$), then an update in $\boldsymbol{w}_1^k$ occurs as follows:

$$\boldsymbol{w}_1^{k+1} = \boldsymbol{w}_1^k + \beta\, \mathrm{e}^{-\gamma r_{\mathrm{f}}^2}(\boldsymbol{w}_2^k - \boldsymbol{w}_1^k) + \alpha(\mathrm{rand} - 0.5) \tag{7}$$

r_{f} represents the Euclidean distance between $\boldsymbol{w}_1^k$ and $\boldsymbol{w}_2^k$, α represents the attractiveness between particles at initial stage, β is a positive constant, γ is the absorption co-efficient of the medium, and rand is the uniform random number generator. The third term α (rand – 0.5) is added for randomisation with α being the randomisation parameter [13].
(b) After comparison of the fitness of all M particles, the particle with the highest fitness is selected; which represents the optimal weighting vector of the kth iteration.

ii. FSS:
(a) If ($P_{\mathrm{d}}[\boldsymbol{w}_m^k] > P_{\mathrm{d}}[\boldsymbol{w}_m^{k-1}]$), then $\boldsymbol{w}_m^k$ is updated as [14]

$$\boldsymbol{w}_m^k = \frac{P_{\mathrm{d}}[\boldsymbol{w}_m^k] - P_{\mathrm{d}}[\boldsymbol{w}_m^{k-1}]}{\max|P_{\mathrm{d}}[\boldsymbol{w}_m^k] - P_{\mathrm{d}}[\boldsymbol{w}_m^{k-1}]|} \tag{8a}$$

(b) After all particles have moved individually, a weighted average of individual movements based on the instantaneous success of all particles is computed and added to the current particle position given as [14]

$$\boldsymbol{w}_m^k = \boldsymbol{w}_m^{k-1} + \frac{\sum_{m=1}^{M} \Delta \boldsymbol{w}_m P_{\mathrm{d}}[\boldsymbol{w}_m^k] - P_{\mathrm{d}}[\boldsymbol{w}_m^{k-1}]}{\sum_{m=1}^{M} P_{\mathrm{d}}[\boldsymbol{w}_m^k] - P_{\mathrm{d}}[\boldsymbol{w}_m^{k-1}]} \tag{8b}$$

where $\Delta \boldsymbol{w}_m = \boldsymbol{w}_m^k - \boldsymbol{w}_m^{k-1}$ shows the displacement of particle due to individual movement in step (a). This step ensures that those particles who had successful individual movements influence the search direction more than other ones.

iii. PSO:
(a) Initialise the particle's velocity ($\boldsymbol{v}_m^k$)$\epsilon[-v_{\max}, +v_{\max}]$, where $v_{\max}$ and $v_{\min}$ represent the maximum and minimum values of velocities.
(b) The local best particle ($\boldsymbol{w}_{\mathrm{l}}^k$) is evaluated in each iteration, which has the highest fitness compared to others. Similarly, the global best particle ($\boldsymbol{w}_{\mathrm{g}}^k$) is selected in each iteration, which possesses the maximum fitness value among all local best particles. The update in ($\boldsymbol{w}_{\mathrm{m}}^k$) and ($\boldsymbol{v}_{\mathrm{m}}^k$) given as [15]

$$\boldsymbol{v}_{\mathrm{m}}^k = c_1 \boldsymbol{v}_{\mathrm{m}}^{k-1} + c_2 \zeta(\boldsymbol{w}_{\mathrm{l}}^{k-1} - \boldsymbol{w}_{\mathrm{m}}^{k-1}) + c_3 \eta(\boldsymbol{w}_{\mathrm{g}}^{k-1} - \boldsymbol{w}_{\mathrm{m}}^{k-1}) \tag{9}$$

$$\boldsymbol{w}_{\mathrm{m}}^k = \boldsymbol{w}_{\mathrm{m}}^{k-1} + \boldsymbol{v}_{\mathrm{m}}^k \tag{10}$$

where ζ and η are uniform random variables between 0 and 1, c_1, c_2, and c_3 are positive constants, which are selected by the practitioner to control the behaviour and efficiency of the PSO. The selection of the parameters is explained in detail in Section 4.1.

Step 4: If it reaches maximum generation, terminate the spectrum sensing algorithm and assign the optimal $\boldsymbol{w}$ to the spectrum allocation module; else, go to step 2.

3.2 Spectrum allocation

The optimal value of weighting vector $\boldsymbol{w} = [w_1, w_2, \ldots, w_D]$, evaluated using FFA, FSS, and PSO in Section 3.1 plays a vital role for conflict free spectrum allocation in this section. The

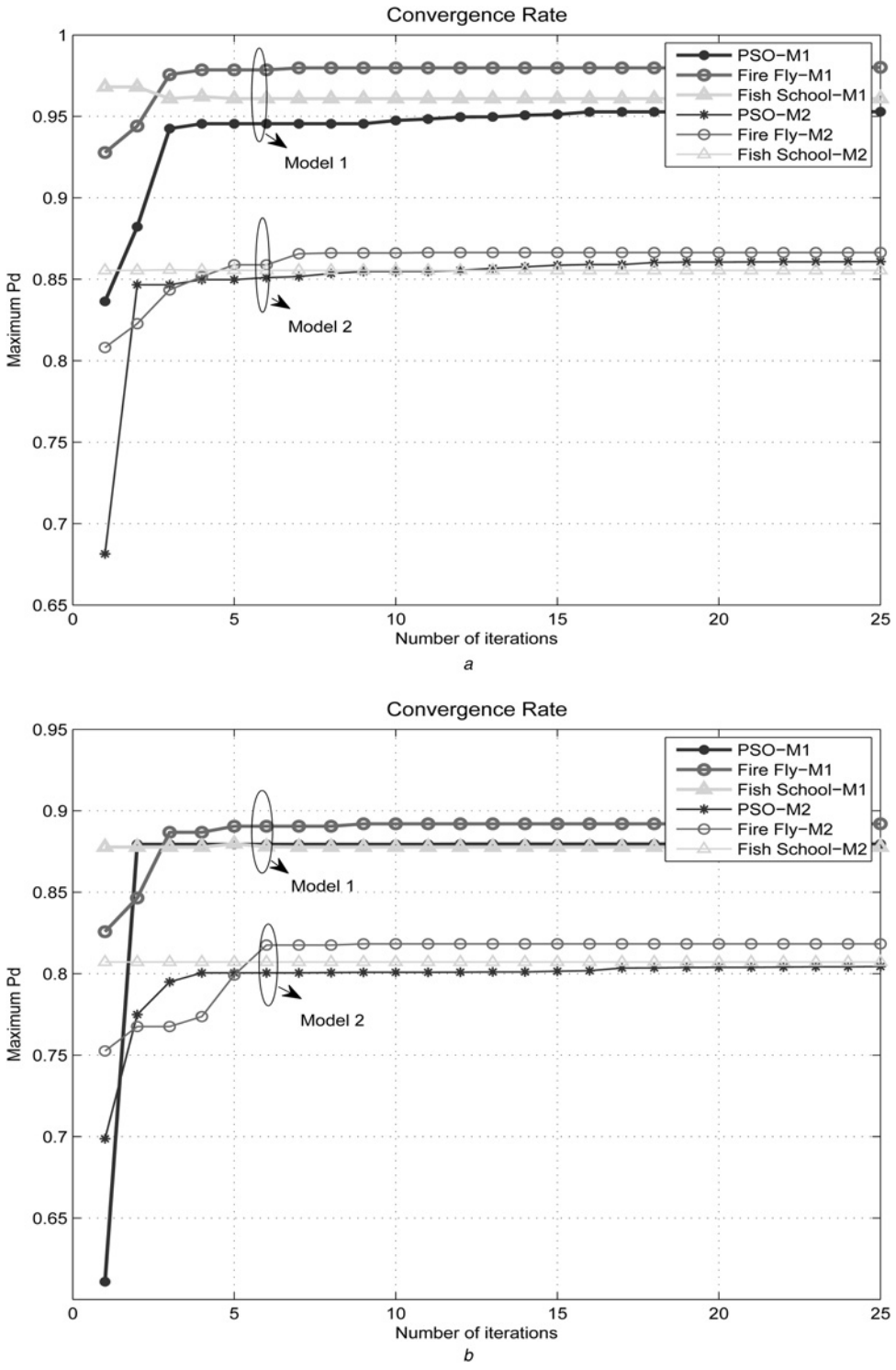

Fig. 2 *Using $P_f = 0.1$, the convergence rate of*

a Rectangular pulse using model 1 (M1) and model 2 (M2)
b Cosine pulse using model 1 (M1) and model 2 (M2)

spectrum allocation of CR can be explained with channel availability matrix, channel reward matrix, and conflict free assignment matrix. It is assumed that D CRs needs to communicate, and U idle channels can be used, where $d = [1, 2, \ldots, D]$ and $u = [1, 2, \ldots, U]$. As CRs sense M channels, so we assume that U out of M channels are vacant. The concerned matrices are defined as:

- *Channel availability matrix (**L**):* $\boldsymbol{L} = l_{d,u} \in [0, 1]$, i.e. $\boldsymbol{D} \times \boldsymbol{U}$ matrix, where $l_{d,u} = 1$, if channel u can be utilised by cognitive user d otherwise $l_{d,u} = 0$.

- *Conflict free channel assignment matrix (**A**):* The conflict free channel assignment matrix $\boldsymbol{A} = a_{d,u} \in [0, 1]_{D*U}$, is a $\boldsymbol{D} \times \boldsymbol{U}$ matrix where $a_{d,u} = 1$, if channel u is assigned to user d or $a_{d,u} = 0$ otherwise.

For conflict free assignment, we propose *assignment precedence matrix* ($\boldsymbol{C}$), i.e. $\boldsymbol{D} \times \boldsymbol{U}$ matrix. Each row in $\boldsymbol{C}$ represents is given by

$$C_d = w_d * L_{d,u} \tag{11}$$

where the product of each row d in L is multiplied with

IET Commun., 2015, Vol. 9, Iss. 16, pp. 1949–1959

corresponding component of optimal $\boldsymbol{w}$ as shown in Fig. 1. During sensing, e.g.; if $w_d > w_{d+1}$, then more precedence is given by the fusion centre to the dth radio. Similarly in spectrum allocation, if two radio users try to access the same channel, then the conflict is resolved by assigning the channel to the specific radio user, who has higher value of w_d.

• *Channel reward matrix (**T**):* The channel reward matrix $\boldsymbol{T} = t_{d,u}$ is a $\boldsymbol{D} \times \boldsymbol{U}$ matrix where $t_{d,u}$ represents the reward attained by user d for utilising channel u. The reward attained by user d for utilising channel u is r_d, i.e. given by

$$r_d = \sum_{u=1}^{U} a_{d,u} * t_{d,u} \tag{12}$$

By following the above model, the spectrum allocation problem can be defined as the optimisation problem that is dependent on the optimisation of r_d. The objective functions considered in this model for optimised spectrum allocation are (a) maximum proportional fair (MPF) reward:

$$\text{MPF} = \left(\prod_{d=1}^{D} r_d + 10^{-6} \right)^{1/D}$$

Maximum sum reward (MSR) $\text{MSR} = \sum_{d=1}^{D} r_d$ and max–min-reward (MMR): $\text{MMR} = \min_{1<=d<=D} r_d$. The performance analysis is given in Section 4.

4 Numerical results and discussion

4.1 Parameter selection for bio-inspired algorithms

The convergence speed and optimisation accuracy of the bio-inspired algorithms is affected by the choice of parameters [16]. For FFA, β represents the attractiveness and for most cases $\beta = 1$ and $\alpha \epsilon [0, 1]$. The parameter γ characterises the variation of the attractiveness, and its value is crucially important in determining the convergence speed and behaviour of FFA. Thus, in most applications, it typically varies from 0.01 to 100 [13]. Following the constraints in [13], we have chosen $\alpha = 1$, $\beta = 1$, and $\gamma = 1.3$. The parameters c_2 and c_3 are the learning parameters or acceleration constants in PSO. A traditional way of improving the PSO method is by manually changing its behavioural parameters. We have used the standard version of PSO with the learning parameters $c_2 \simeq c_3 \simeq 2$ [17, 18]. Various studies have been reported in the literature [19, 20] regarding the choice of the inertia weight (c_1) and the velocity boundaries in PSO, which is believed to influence the degree of exploration versus exploitation. After conducting extensive survey and experiments, it is recommended in [21] that $c_1 \epsilon [-2, 2]$ and $v_m^k \epsilon [-4, 4]$ for optimisation experiments. Following [21], we have chosen $c_1 = 1$ and $v_m^k = [-2, 2]$. Similarly in [8], the effect of non-linear distortion produced by HPAs on the performance of multiple input and multiple output system is analysed using different values of e_A and f_A. Following [8], we have chosen $e_A = 1$ and $f_A = 0.25$, for HPA model (model 1). The sum of coefficients of memory less polynomial model (model 2) are assumed to be unity, so we set b_p coefficients as 0.4, 0.2, and 0.4, where $P = 3$. For our initial analysis, we assume the number of particles as $M = 15$, the number of radios as $D = 7$, where the received SNR of each radio is in range of [0, −5] dB given as: 0, −0.75, −1.5, −2.25, −3, −3.75, and −4.5 dB. We have also analysed different values of D and SNR in Sections 4.4 and 4.5, respectively.

4.2 Comparison of PSO, FFA, and FSS

i. *Non-linear signals:* In order to compare the convergence performances of the bio-inspired algorithms, the relationship between the 'number of iterations' and the maximum value of 'P_d' is demonstrated in Fig. 2, by setting $P_f = 0.1$. A rectangular pulse is considered in Fig. 2*a* as the input pulse and undergoes non-linear distortion using model 1 and model 2, whileFig. 2*b* deals with cosine pulse. The results have shown that FFA outperformed PSO and FSS for both non-linear models. The maximum value of P_d attained by PSO, FFA, and FSS for rectangular pulse: using model 1 is 0.9709, 0.9749, 0.9623 and using model 2 is 0.8528, 0.8632, 0.8565, respectively. However, the maximum value of P_d attained by PSO, FFA, and FSS for cosine pulse: using model 1 is 0.9424, 0.9760, 0.9615 and using model 2 is: 0.8491, 0.8602, 0.8555, respectively. It is observed that model 1 performed better than model 2 for both input pulses. The difference in performance of model 1 and model 2 is due to the nature of non-linear functions involved in the system.

ii. *Linear signals:* We have also considered both rectangular and cosine pulses without non-linearities in Fig. 3. It was observed that FFA outperforms PSO and FSS again. The maximum value of P_d attained by PSO, FFA, and FSS for rectangular pulse is 0.9722, 0.9754, and 0.9630, while the maximum P_d value attained by PSO, FFA, and FSS for cosine pulse is 0.9259, 0.9432, and 0.9234, respectively. The value of P_d for linear signals is higher than non-linear signals. The non-linear distortions induced by model 1 and model 2 are responsible for the P_d degradation in non-linear signals.

4.3 Comparison of bio-inspired algorithms with WLC

The convergence of bio-inspired algorithms is examined for fixed values of P_f in Figs. 2 and 3. However, in real scenarios, P_f can change anytime so the effect of a changing value of the P_f on P_d is plotted as the ROC curve in Figs. 4*a* and *b*. The value of P_f is changed in each iteration by setting its $P_f = 0.01$ in the first iteration and incremented by a value of $P_f = 0.01$ in each iteration. The performance of WLC is compared with bio-inspired techniques and the results have shown that all three bio-inspired algorithms outperform the WLC method.

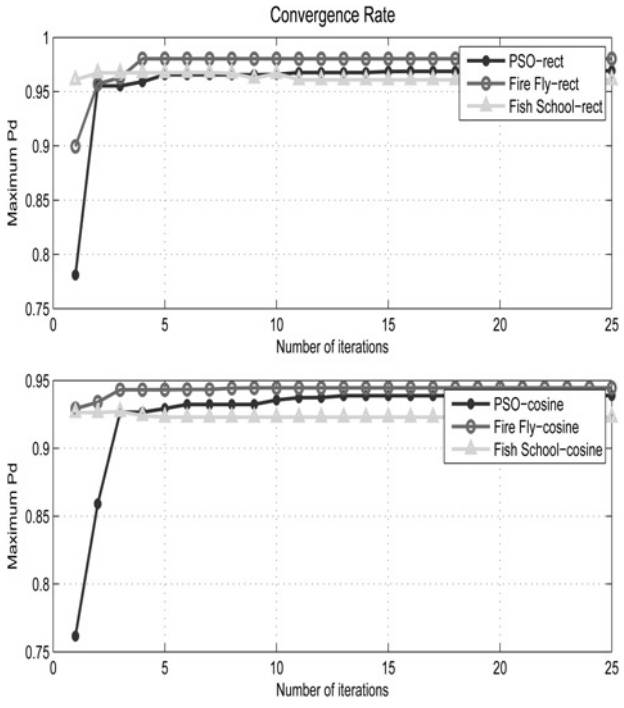

Fig. 3 *Using $P_f = 0.1$, the convergence rate of linear rectangular and cosine pulses*

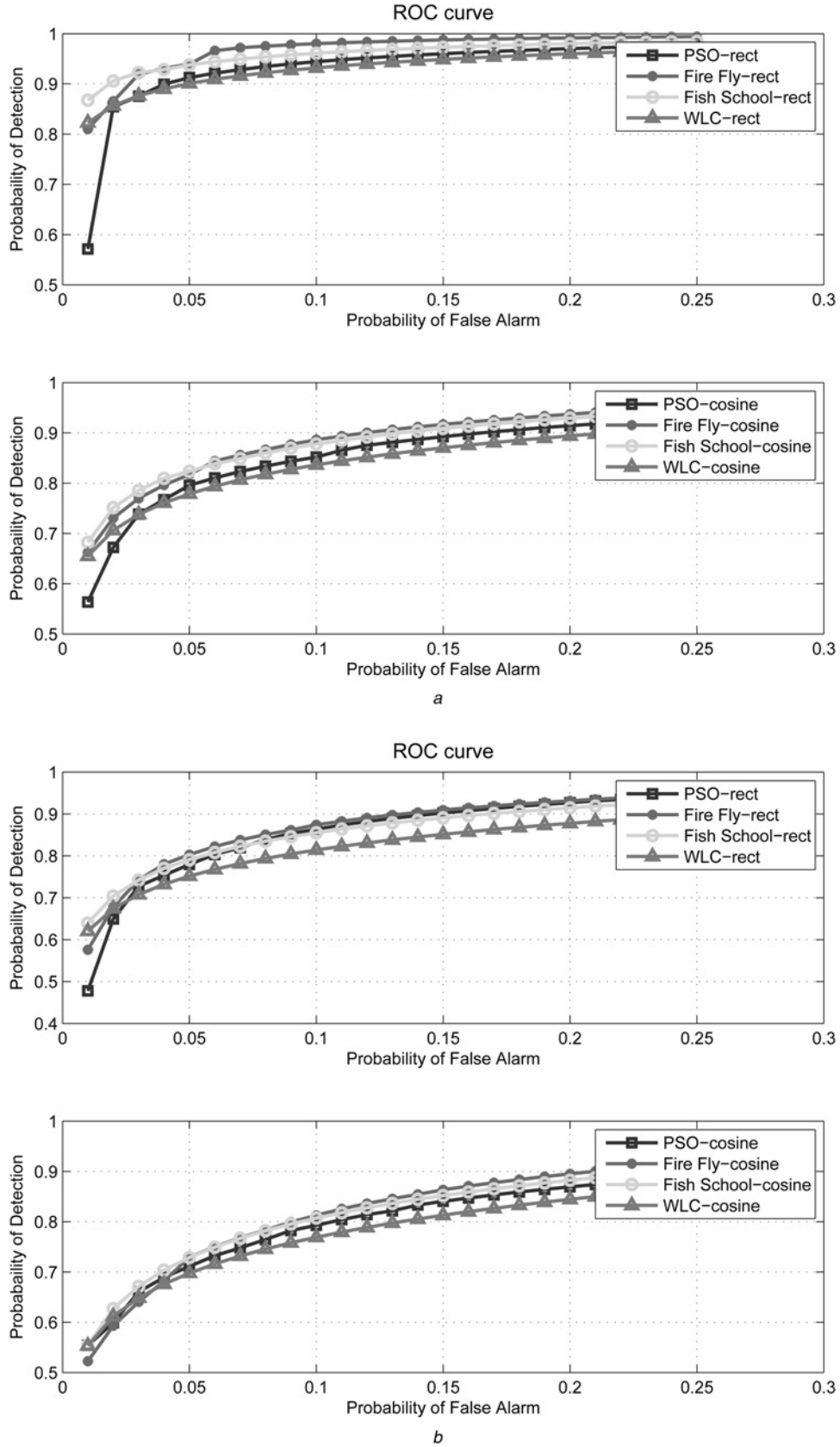

Fig. 4 *Comparison of rectangular and cosine pulses for different values of P_f using*

a Model 1 (M1)
b Model 2 (M2)

4.4 Effect of SNR

In the above subsections, different values of SNR for each radio are used while keeping the SNR for an individual radio constant for all simulation runs. The effect of different SNR sets is demonstrated in Fig. 5*a*, where SNR set 1 is assumed to be the same as mentioned in Section 4.1. SNR set 2 is assumed as: −5.25, −6, −6.25, −7, −7.75, −8.5, and −9.25 dB. It was

IET Commun., 2015, Vol. 9, Iss. 16, pp. 1949–1959

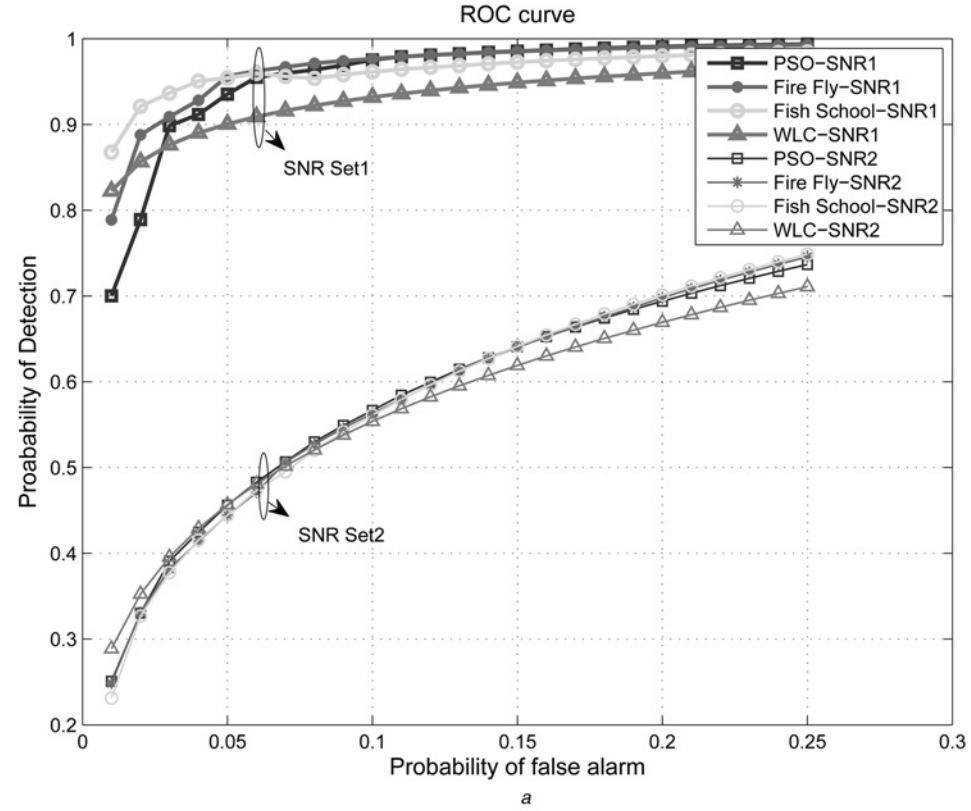

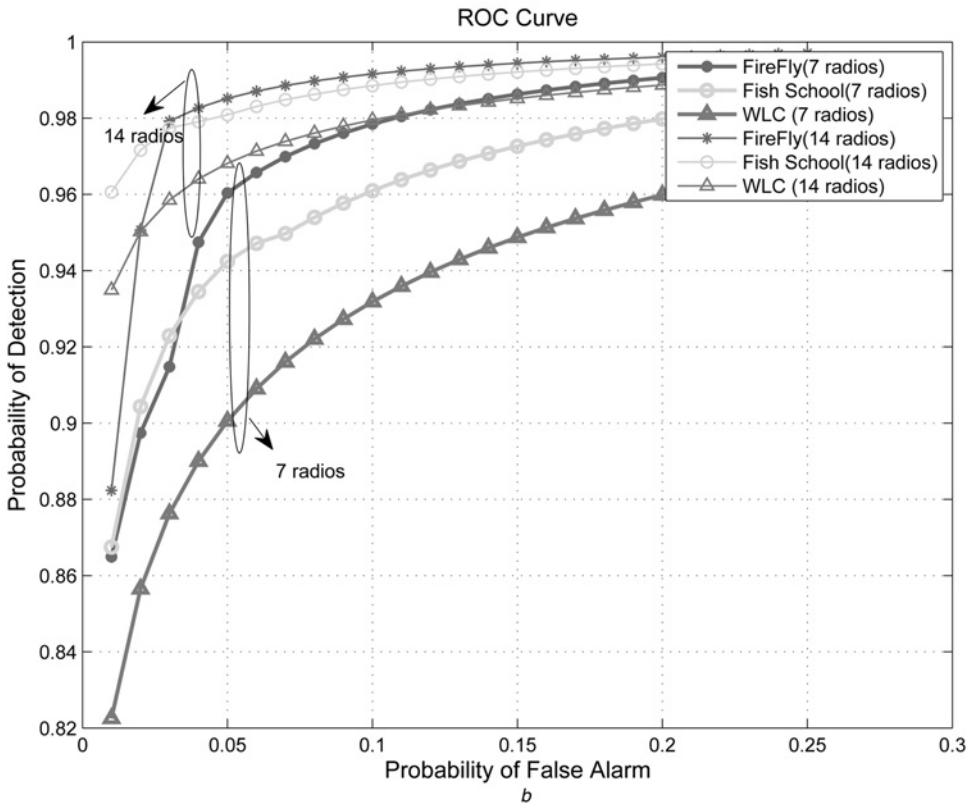

Fig. 5 *Effect of*

a Different values of SNR on the value of P_d
b Changing the number of radios on the value of P_d

observed that the performance of SNR set 2 is low compared to SNR set 1. This is because SNR set 2 ranges between [−5, −10] dB, while SNR set 1 ranges between [0, −5] dB. As P_d is directly proportional to SNR, so the value of P_d increases with an increase in the value of SNR for each radio.

4.5 Effect of the number of radios

We have checked the effect of increasing the number of CR's from $D = 7$ to $D = 14$ in Fig. 5*b*, where the SNR of $D = 14$ also lies in the range [0, −5] dB as $D = 7$ explained above. By increasing D, we

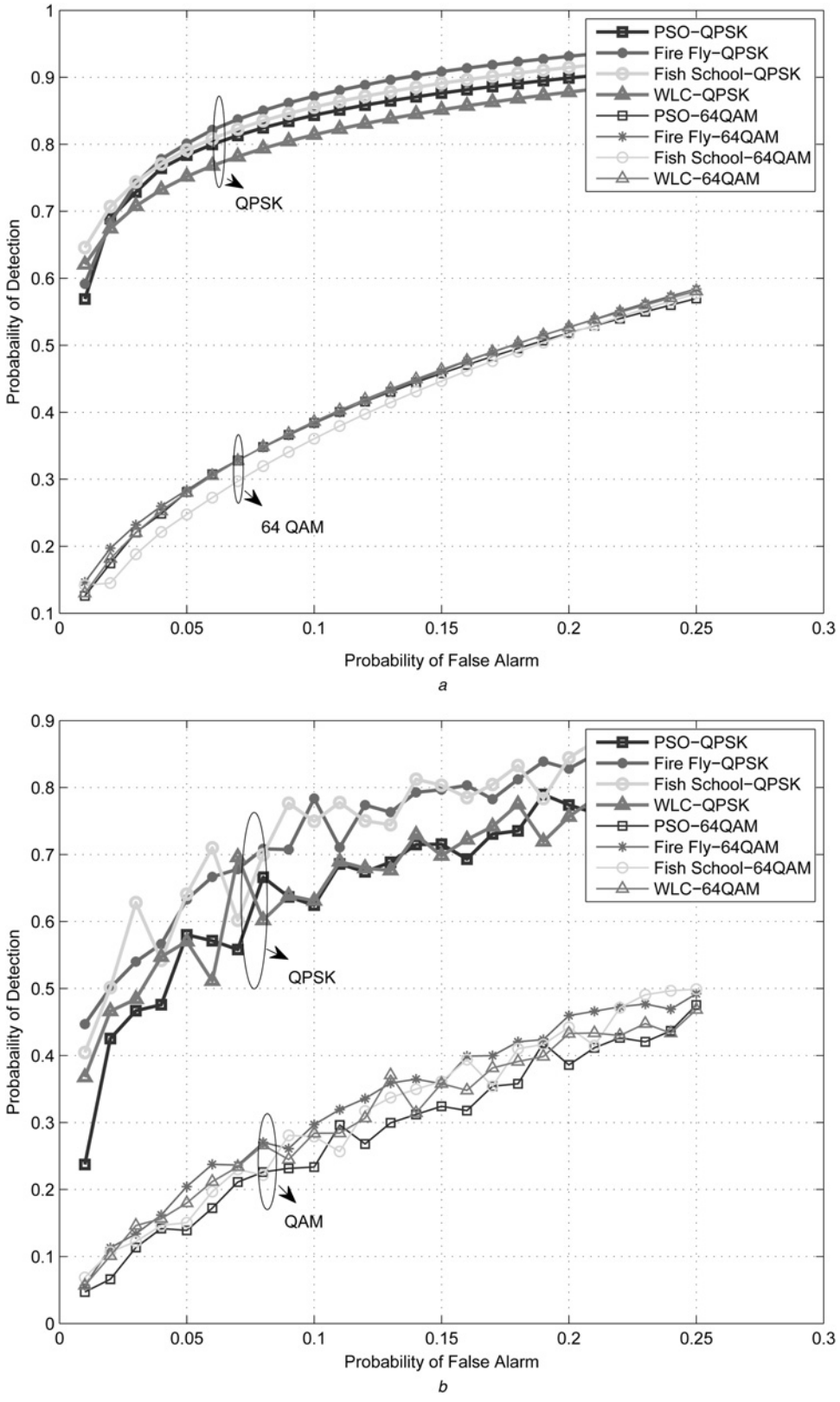

Fig. 6 *Effect on the value of* P_d *using*

a Different modulation schemes (QPSK and QAM)
b Modulation schemes plus interference

actually increase the dimensions of particle's position, which eventually results in better performance. It is observed in Fig. 5*b*, that FFA and FSS outperforms WLC for both cases, $D = 7$ and $D = 14$. Though increase in the number of radios, increases the mean P_d value for all algorithms, however, it results an increase in the computational time and memory as well. Using MATLAB on a system with Core i7 system and 8 GB RAM, we found that the occupied memory and execution time for $D = 7$ is 964 MB and 15.9 s, respectively, however, the occupied memory and execution time for $D = 14$ is 975 MB and 20.6 s, respectively.

IET Commun., 2015, Vol. 9, Iss. 16, pp. 1949–1959

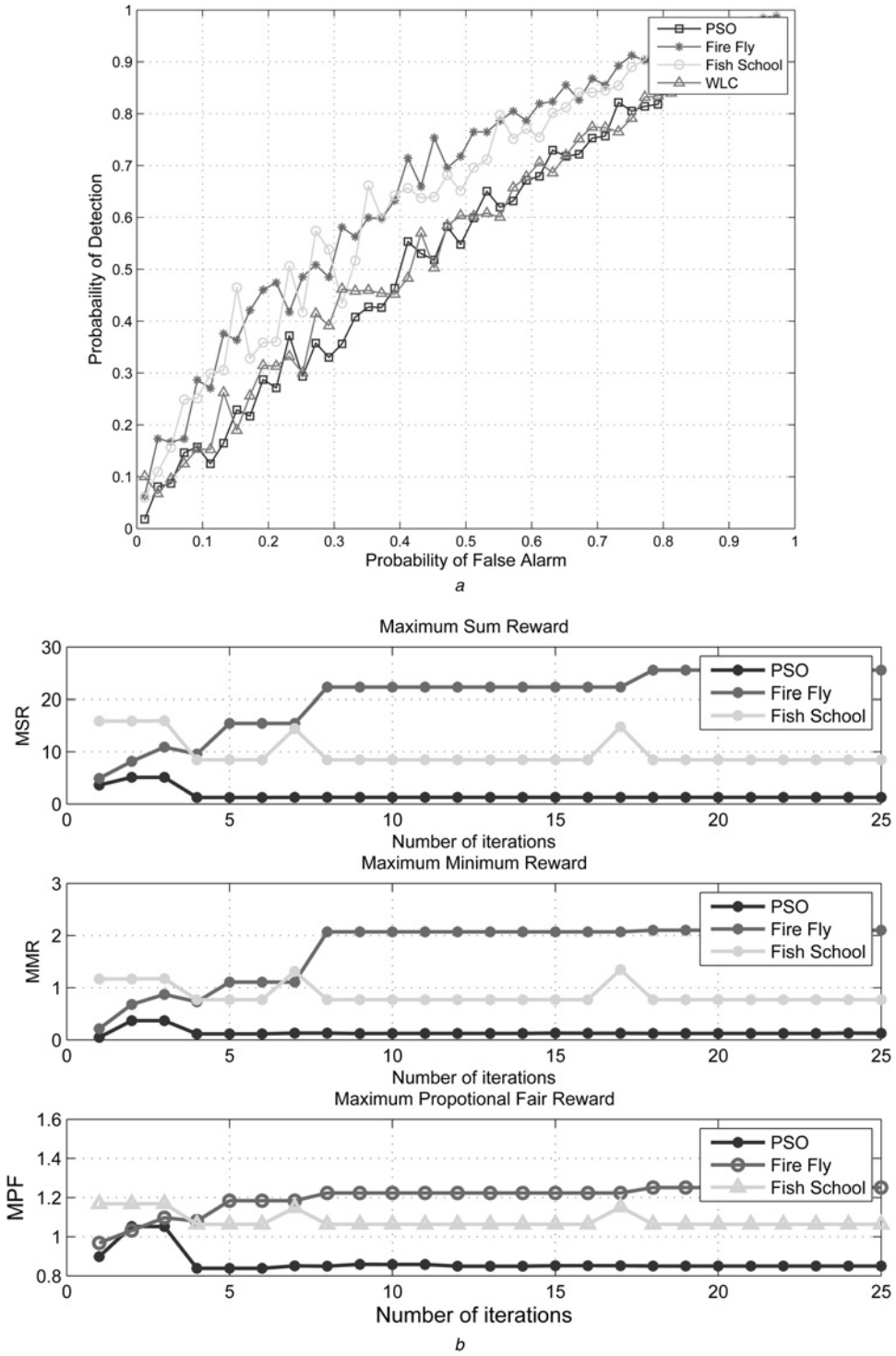

Fig. 7 *Effect on*

a Modulated QPSK signal passed through non-linear frequency selective faded model using k = 205
b Spectrum allocation rewards using rectangular pulse and model 2

4.6 Effect of modulation, interference and fading

We have considered two modulation schemes [64 quadrature amplitude modulation (QAM) and quadrature phase shift keying (QPSK)] for analysing the case, when $I(m)$ is fed into a non-linear amplifier as modulated input. The result is shown in Fig. 6*a* using rectangular input pulse. It is observed in Fig. 6*a*, that modulated rectangular pulse using QPSK attains higher P_d than 64 QAM. The FFA has outperformed other algorithms, but there is 11% decrease in the value of its P_d compared to the non-linear model 2 without modulation.

Further, we introduce external interference following the model in [6] to the non-linear model modulated using QPSK and 64 QAM. The interference represents the noise faced by each CR caused due to PU's. It is observed in Fig. 6*b*, that the value of P_d decreases more with the introduction of interference. The degradation in the value of P_d occurs because $r_d(m)$ faces both white Gaussian noise and interference in the channel. It is again observed that FFA has outperformed other schemes, but interference degrades the performance of FFA 10% more compared to non-linear modulated model mentioned above.

Table 2 Performance comparison of linear, non-linear, non-linear modulated, and non-linear modulated faded models

Performance comparison												
	Algorithm	Linear model			Model 2			A = model 2 + QPSK			A + fading		
		MPF	P_d	T'	MPF	P_d	T'	MPF	P_d	T'	MPF	P_d	T'
$k=25$, $D=7$	PSO	0.87	0.91	0.62	0.79	0.83	0.63	0.77	0.71	2.09	0.71	0.48	30.9
	fire fly	1.19	0.97	0.71	1.11	0.86	0.72	1.06	0.79	2.91	0.91	0.62	35.1
	fish school	1.07	0.95	0.64	1.01	0.85	0.69	0.99	0.75	2.11	0.91	0.52	32.5
$k=45$, $D=7$	PSO	0.88	0.94	0.91	0.81	0.81	1.15	0.76	0.71	3.75	0.74	0.46	54.5
	fire fly	1.27	0.98	0.99	1.25	0.88	2.11	1.09	0.73	4.01	0.93	0.53	60.5
	fish school	1.11	0.96	0.94	1.09	0.86	1.71	1.06	0.72	3.91	0.42	0.66	55.1
$k=25$, $D=10$	PSO	0.93	0.97	0.67	0.85	0.84	0.68	0.80	0.77	3.41	0.75	0.55	132.5
	fire fly	1.20	0.98	0.87	1.17	0.87	0.95	1.09	0.80	8.62	0.97	0.69	160.2
	fish school	1.15	0.97	0.69	1.07	0.86	0.64	1.01	0.70	3.56	0.94	0.60	130.5
$k=45$, $D=10$	PSO	0.97	0.98	0.97	0.87	0.87	0.92	0.80	0.60	4.35	0.77	0.54	159.7
	fire fly	1.38	0.98	0.97	1.29	0.88	1.74	1.18	0.68	15.2	0.98	0.58	288.1
	fish school	1.20	0.97	0.98	1.16	0.87	1.32	1.12	0.76	3.84	0.99	0.57	155.1

Further, Fig. 7*a* analyses the effect of frequency selective fading channels for the non-linear modulated model with interference mentioned above. We considered the channel impulse response (G_d) modelled as T time delayed taps with independent Rayleigh fading gains [22] for 250 iterations. We considered QPSK as the modulation schemes. The mean P_d values attained by PSO, FFA, FSS, and WLC are 0.5519, 0.6704, 0.6506, and 0.5615, respectively. The performance of FFA is decreased 7% more with the introduction of fading, however, the execution time increases compared to all models. The time required for 250 iterations is 1 h (3545.35 s). The detailed comparison of these models is presented in Table 2.

4.7 MPF reward

The spectrum allocation objective function: MSR, MMR, and MPF are plotted in Fig. 7*b* using model 2, where the rectangular pulse is used as an input primary signal. The mean MSR attained by PSO, FFA, and FSS are 1.6641, 20.2950, and 9.8550, respectively, while MMR is 0.1404, 1.7332, and 0.8628, respectively, and MPF is 0.8678, 1.1987, and 1.0831, respectively. It was observed that FFA outperformed FSS and PSO for all three objective functions.

4.8 Performance comparison

We have compared the performance of linear, non-linear, non-linear modulated, and non-linear modulated faded primary user signals in Table 2. We have chosen mean MPF, mean P_d, and T' as the performance metric, where T' represents the total time required by iterations: $k=25$ or $k=45$. The time required by each iteration (t'') can be calculated using $t''=T'/k$. It was observed that increase in the value of radio users ($D=7$ to $D=10$) increases the value of P_d, MPF and computational time for all iterations. It was also observed that linear signals have higher P_d, MPF and computational cost compared to the non-linear signals. The value of P_d, MPF decreases and the computational cost increases as we move from a linear model to faded model (the left side to the right side) in Table 2 due to the increase in losses and distortions faced by the input signals.

5 Discussion and conclusion

We have presented a framework for CSS and allocation in CRs using used bio-inspired techniques. We have considered both linear and non-linear signals. It was observed that the non-linearities induced using HPA model degrades the performance of spectrum sensing more compared to memory less polynomial model.

We also found that all bio-inspired techniques performed equally well in the presence of Gaussian noise and outperformed the conventional spectrum sensing weighting method: WLC. Bio-inspired techniques performed better because they are the iterative search processes which efficiently find near optimal solutions using exploration and exploitation principles. However, we observed that bio-based solutions and WLC are affected by the change in SNR values. The increase in noise, interference, and fading degrades the performance of all algorithms. PSO is affected more compared to FFA, because FFA is potentially more powerful in solving noisy non-linear optimisation problems compared to PSO. Similarly FSS auto-regulates its exploitation and exploration capabilities compared to PSO, so we found that FSS performed better in noisy conditions compared to PSO, but its performance is worse than FFA.

We have also developed a precedence-based spectrum allocation framework which is dependent on spectrum sensing weighting vector. It was found that bio-inspired techniques not only help to attain higher value of probability of detection, but also ensure conflict free spectrum allocation. The collaboration between different fusion centres will be studied as a future work for improving the performance of the system.

6 Acknowledgment

Yunfei Chen acknowledges the support of the Open Project Fund (ICT1517), the State Key Laboratory of Industrial Control Technology, Zhejiang University, China.

7 References

1 Chen, Y.: 'Collaborative spectrum sensing in the presence of secondary user interference for lognormal shadowing', *J. Wirel. Commun. Mob. Comput.*, 2012, **12**, (10), pp. 463–472
2 Chavali, V.G., Dasilva, C.R.: 'Collaborative spectrum sensing based on new SNR estimation and energy combining method', *IEEE Trans. Veh. Technol.*, 2011, **60**, (8), pp. 4024–4029
3 Yucek, T., Arslan, H.: 'A survey of spectrum sensing algorithms for cognitive radio applications', *IEEE Commun. Surv. Tutorials*, 2009, **11**, (1), pp. 116–130
4 Peng, C., Zheng, H., Zhao, B.: 'Utilization and fairness in spectrum assignment for opportunistic spectrum', *ACM J. Mob. Netw. Appl.*, 2006, **11**, (4), pp. 555–576
5 Liao, C., Chen, J., Youxi, T.: 'Parallel algorithm of spectrum allocation in cognitive radio', *J. Electron. Inf. Technol.*, 2007, **29**, (7), pp. 1068–1611
6 Dikmese, S., Srinivasan, S., Shaat, M., *et al.*: 'Spectrum sensing and resource allocation for multicarrier cognitive radio systems under interference and power constraints', *EURASIP J. Adv. Signal Process.*, 2014, **12**, doi: 10.1186/1687-6180-2014-68, pp. 1–12
7 Ghazaany, T.S.: 'Design and implementation of adaptive base band predistorter for OFDM nonlinear transmitter'. PHD Thesis, University of Bradford, UK, 2011
8 Chi, D.W., Das, P.: 'Effects of nonlinear amplifiers and narrow band interference in MIMO-OFDM with Application to 802.11n WLAN'. Proc. Int. Conf. on Signal Processing and Communication Systems, December 2008, pp. 1–7
9 Saleh, A.A.M.: 'Frequency-independent and frequency-dependent nonlinear models of TWT amplifiers', *IEEE Trans. Commun.*, 1981, **29**, (11), pp. 1715–1720
10 Quan, Z., Sayed, A.H.: 'Optimal linear cooperation for spectrum sensing in cognitive radio networks', *IEEE J. Sel. Top. Signal Process.*, 2008, **2**, (1), pp. 28–40

11 Lohrer, M.F.: 'A comparison between the firefly algorithm and particle swarm optimization'. Thesis, Oakland University, USA, 2013
12 Cavalcanti-Junior, G.M., Bastos-Filho, C.J.A., Lima-Neto, F.B., *et al.*: 'A hybrid algorithm based on fish school search and particle swarm optimization for dynamic problems'. Advances in Swarm Intelligence, 2011 (*LNCS*, 6729), pp. 543–552
13 Yang, X.: 'Firefly algorithms for multimodal optimization', *Lect. Notes Comput. Sci.*, 2009, **5792**, pp. 169–178
14 Filho, A.B., De Lima Neto, F.B.: 'A novel search algorithm based on fish school behavior'. IEEE Int. Conf. on Systems, Man and Cybernetics, 2008, pp. 2646–2651
15 Poli, R., Kennedy, J., Blackwell, T.: 'Particle swarm optimization', *J. Swarm Intell.*, 2007, **1**, (1), pp. 33–57
16 Yang, X.: 'Nature – inspired metaheuristic algorithms' (Luniver Press, UK, 2010, 2nd edn.)
17 Kennedy, J., Eberhart, R.C.: 'Particle swarm optimization'. Proc. of IEEE Int. Conf. on Neural Networks, Piscataway, NJ, pp. 1942–1948
18 Kennedy, J., Eberhart, R., Shi, Y.: 'Swarm intelligence' (Academic Press, London, 2001)
19 Shi, Y., Eberhart, R.: 'Parameter selection in particle swarm optimization'. Proc. Evolutionary Programming, VII (EP98), 1998
20 Eberhart, R., Shi, Y.: 'Comparing inertia weights and constriction factors in particle swarm optimization', *Proc. Congr. Evol. Comput.*, 2000, **1**, pp. 84–88
21 Erik, M., Pedersen, H.: 'Good parameters for particle swarm optimization'. Technical Report no. HL1001, Hvass Laboratories, 2010
22 Jain, R.: 'Channel models', A tutorial(2007)', http://www.cse.wustl.edu/jain/cse574-08/ftp/channel_model_tutorial.pdf, Accessed 12 January 2014